Regenerated Spider Silk: Processing, Properties, and Structure

Andreas Seidel,[†] Oskar Liivak,[†] Sarah Calve,[†] Jason Adaska,[†] Gending Ji,[†,‡] Zhitong Yang,[†] David Grubb,[‡] David B. Zax,[§] and Lynn W. Jelinski*[,⊥]

Center for Advanced Technology in Biotechnology, Department of Materials Science and Engineering, and Department of Chemistry and Chemical Biology, Cornell University, Ithaca, New York 14853, and Chemistry Department, Louisiana State University, 240 T. Boyd Hall, Baton Rouge, Louisiana 70803

Received June 4, 1999; Revised Manuscript Received November 23, 1999

ABSTRACT: Spider dragline silk is Nature's high-performance protein fiber. This biomaterial has attracted much interest from scientists in various disciplines since it has become feasible to produce spider silk proteins by means of biotechnology. This article reports on research directed toward the regeneration of spider silk. A procedure is described—including spinning and postspinning processing—that produces fibers with promising mechanical properties from dissolved natural spider dragline silk. Tensile tests and structural characterization of the regenerated fibers illustrate correlations between the macroscopic and microscopic properties of the final material and between these properties and the fiber's processing history. Results point to the importance of an aqueous environment in the annealing of structure. The revealed structure−property relationships are expected to be of fundamental importance for the future design of man-made protein products.

Introduction

Nature can provide us with many lessons about environmentally friendly technologies and futuristic materials with improved properties. Even at an early stage, biomimetics—the art of mimicking biological structures and processes—has led to a variety of interesting biomaterials with a broad field of applications.[1] Proteins, in particular, have been identified as a promising basis for a diverse class of novel high-performance structural polymer materials. Models for man-made protein and protein-like compounds include collagen—a major component of mammalian connective tissue and bones—and silks—produced by both insects and spiders for a variety of functions. Collagen-based materials and composites are already exploited commercially for medical applications such as tissue replacement, bone repair, wound dressings, and surgical sutures.[1] The exploitation of silks and silk-like polymers beyond the traditional use of silkworm silk in textile fabrics, however, remains a challenge.[1,2]

Spider silk is a particularly promising material. Its outstanding mechanical properties are superior even to those of silkworm silk.[1,3] Recent successes in the identification, artificial synthesis, and expression of genes coding for spider silk proteins[4−12] have spurred interest in the relationships between the molecular structure and the functional behavior of spider silks.[3,13−15] They have further opened the possibility of biotechnology-based large-scale production of spider silk proteins and of rationally designed materials inspired by these biopolymers. Laboratory-scale expression of silk proteins is now feasible, in both bacteria and yeasts,[7−12] and there has even been a recent proposal to express silk genes in mammalian species.[16]

A challenging avenue of research remains in learning how to process the raw protein powder into marketable structural materials, such as fibers. As a starting point, we have chosen to focus our fundamental studies on the regeneration of natural silk materials as the native fibers, and their properties can serve, in this case, as benchmarks for the evaluation of the laboratory-based processing. Wet-spinning of silk and silk-like proteins into fibers has recently been described by several groups.[8,12,17−21] While most of the previous work has aimed at regenerating fibers from solubilized silkworm silk,[18−20] the present study reports on our recent progress in regenerating and processing fibers from dissolved natural spider silk. Scanning electron microscopy (SEM), solid-state ^{13}C nuclear magnetic resonance (NMR) spectroscopy, wide-angle X-ray diffraction (WAXD), and tensile tests were used to characterize the regenerated fibers. The motivation was to reveal correlations between the processing conditions and the microscopic and macroscopic properties of the protein material. The results of this model study on a "wild-type" silk are likely to serve as benchmarks for the future progress on tailoring of genetically modified protein products of this class.

Experimental Section

Spinning and Postspinning Processing. Fibers were regenerated from a 2.5% w/w solution of *Nephila clavipes* major ampullate gland spider silk in hexafluoro-2-propanol. The conditions of the spinning process and of the collection of the native silk were similar to those described in a previous communication.[21] In the present study, blunt point hypodermic stainless steel needles supplied by Vita Needle Co. (Needham, MA) were used as spinnerets. The needles had inner diameters of 150, 175, and 250 μm and a length of $^1/_4$ in. A Luer Lock hub allowed for direct attachment of the needles to disposable syringes containing the spinning dope. The total dead volume of the spinning device was about 100 μL. This value translates into an unavoidable protein loss per spinning run of only 4 mg.

A single filament formed upon extrusion of the silk solution into an ambient temperature acetone bath. After falling freely to the bottom of the spinning container, the filament was

[†] Center for Advanced Technology in Biotechnology, Cornell University
[‡] Department of Materials Science and Engineering, Cornell University
[§] Department of Chemistry and Chemical Biology, Cornell University
[⊥] Chemistry Department, LSU.
* To whom correspondence should be addressed.

10.1021/ma990893j CCC: $19.00
Published on Web 01/11/2000

allowed to coil on itself and to cure in the coagulation bath for 1 h. For postspinning processing, the as-spun filaments were cut into 8 cm long pieces. Those pieces were drawn in air at a speed of approximately 8 cm/s while still wet with acetone and afterward were allowed to dry in air at constrained length. The highest drawing ratio achieved in this processing step without tensile failure of the regenerated fiber was 3.5. Some of the single-drawn, air-dried fibers were free-end annealed for 1 h in a vacuum at 100 °C. Another group of fibers was soaked in water—either constrained or unconstrained in length—and afterward air-dried again or air-dried and further annealed. Soaked with water, the prestretched fibers could be elongated by an additional factor of up to 2.5 in a second drawing step. Hence, with a two-step drawing procedure total drawing ratios (the product of the drawing ratios in both steps) of up to DR = 9 could be realized. The behavior of the material in the second drawing step is observed to improve with increasing time that the prestretched fiber sits in water before any stress is applied.

Fiber Characterization. The mechanical properties of regenerated spider silk fibers were examined at a temperature of 70 °F and a relative humidity of 65% using an Instron tensile testing system. Specimens of 5 mm gauge length were equilibrated for at least 24 h under these environmental conditions and were then stretched to failure at a rate of 2 mm/min. The diameter of the unstrained fiber, measured by optical microscopy, was used to calculate the tensile stress from the applied force. Specimens for SEM observation were attached to an aluminum holder with double-sided electrically conductive carbon tape and then coated with a layer of gold–iridium before transfer into the vacuum chamber of a Leica Stereoscan 440.

Magic angle spinning (MAS) NMR investigations were performed on a home-built multichannel spectrometer with 5 kHz sample spinning. The system operates at a ^{13}C Larmor frequency of 90.556 MHz. After a 2.5 ms $^{13}C-^{1}H$ cross-polarization contact period (with ^{1}H spin-lock field at 60 kHz) spectra were acquired with proton decoupling fields of strength 90 kHz. Free induction decays (FIDs) were accumulated with a 2.5 s repolarization delay. Chemical shifts are reported relative to TMS as the reference.

Wide-angle X-ray diffraction experiments were performed at the D1 beam line of the Cornell High Energy Synchrotron Source (CHESS) using radiation with a wavelength of 0.154 nm and a 1024 × 1024 pixel CCD detector. Fiber bundles were held in frames made from cardboard that were mounted on a rotation stage. Square collimators limited the beam to 0.5 mm. To reduce air scattering, a helium-filled tube took up almost all the distance from the X-ray source to the specimen. Residual air scattering was subtracted from all patterns.

Results and Discussion

The results of the characterization of the regenerated fibers will be presented in four sections. The first two treat the macroscopic fiber properties phenomenologically, by a discussion of the texture and tensile properties. The emphasis here lies on the identification of systematic changes of the material's properties resulting from the postspinning processing (drawing, water treatment, and annealing). The last two sections deal with the microscopic, i.e., molecular-level features, of the regenerated silks, namely the secondary protein structure and the crystallinity and overall molecular orientation of the fibers. The presentation here focuses on correlations between the microscopic and macroscopic fiber properties. The main aim is to draw a molecular-level picture of the fiber changes during the postspinning processing and to determine how these changes affect the material's tensile behavior.

Fiber Texture. The fresh (i.e., unprocessed) regenerated spider silk has a spongy appearance (Figure 1a).

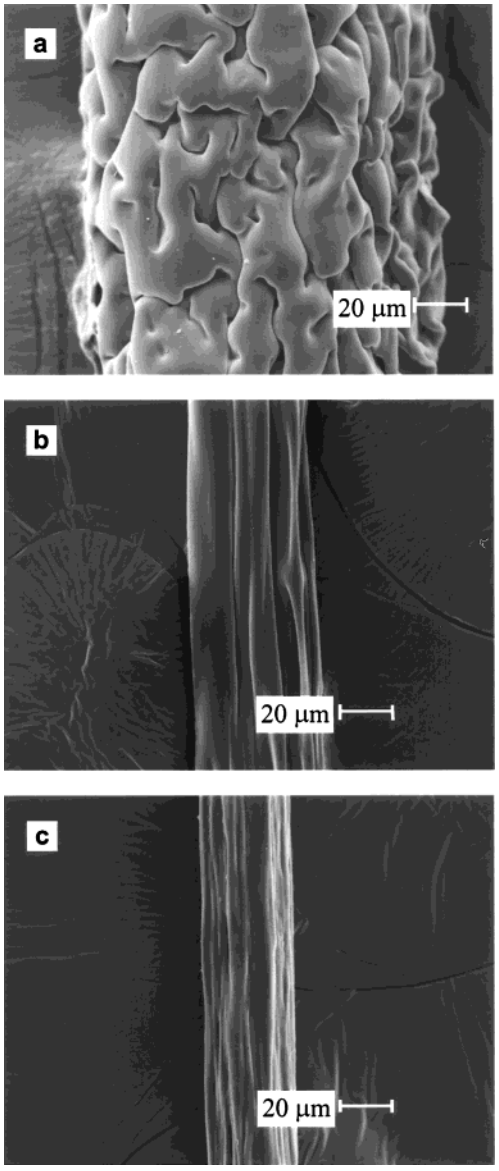

Figure 1. Morphology of regenerated spider silk. Scanning electron micrographs of fibers spun with a 250 μm spinneret: (a) as-spun, (b) single-drawn (DR = 3.5), (c) double-drawn (DR_1 = 3.5, DR_2 = 2).

The average diameters of the as-spun, air-dried, and annealed fibers are nearly twice as large as would be predicted from the size of the spinneret, the protein concentration of the spinning dope, and the density of the native spider silk. From this we conclude that the fresh regenerated silk fibers exhibit a lower density than the native material and hence must be considered very porous. Pores are commonly found in wet-spun fibers. In the precipitation step much of the polymer solvent is trapped in the fiber. On drying, evaporation of this residual solvent leaves the pores behind.

Drawing of the regenerated silk fiber results in a change from a spongy to a fibrillar appearance (Figure 1a,b). This change in appearance is accompanied by a very large decrease in the fiber diameter, suggesting a substantial increase in fiber density. We conclude that the initial drawing of the as-spun fiber causes collapse of the unfavorable pore structure, produced in the course of the wet-spinning process. The relatively small observed decrease in fiber diameter in the second drawing step (compare parts b and c of Figure 1), on the other

hand, is quantitatively balanced by the increase in length of the fiber, so that in this second stage the fiber density remains constant.

Tensile Behavior. The postspinning drawing induces changes not only of the texture but also of the mechanical property profile of the protein fibers. Tensile tests have been performed with about 150 regenerated spider silk samples, covering specimens of all different processing histories. The as-spun fibers are very weak, but both the strength and stiffness of the regenerated silk can be enhanced by 2 orders of magnitude by postspinning drawing. The tensile strengths and moduli of fibers obtained under the same spinning conditions show an exponential dependence on the diameter of the processed specimen (Figure 2). Similar behavior has been reported for regenerated silkworm silks.[20]

In our regenerated fibers, the highest strength measured was 320 MPa, and the best modulus achieved was 8.0 GPa. These values do not yet compete with the mechanical properties of the native silk (strength, 875 MPa; modulus, 10.9 GPa[22,23]). However, extrapolation from the present data (Figure 2) suggests that the spinning scheme we have applied should be capable of generating materials competitive with, or perhaps even superior to, the native silk. This would require higher postspinning drawing ratios allowing for a further decrease in fiber diameter. Remarkably, the double-drawn regenerated silk produced in this study is both stronger and stiffer than fibers prepared by Fahnestock from an artificial, spider silk analogue protein (strength, 140 MPa; modulus, 4.6 GPa[3,12]). While the wet-spinning procedures applied in both investigations are similar, in Fahnestock's study the fiber was not drawn in water. This suggests that the presence of water during the postspinning drawing is of some importance for the improvement of the mechanical properties of protein fibers.

The strength and stiffness of the drawn fibers are not significantly influenced by a postdrawing water treatment at constrained length or by a free-end annealing process. (The mechanical data of specimens with different postdrawing processing histories fall on common lines in Figure 2a,b.) However, where most fibers processed in the absence of water are brittle and break at strains of only 4−8%, the majority of our specimens, which have been in contact with water during the postspinning processing, undergo inelastic deformation to very high strains of up to 100% before failure. Fibers spun into a bath of acetone containing traces of water exhibit higher strength and stiffness than specimens of comparable diameter spun into pure acetone (Figure 2). As the water content of the coagulation bath is increased, the as-spun fibers tend to become sticky. No fiber formation was observed when the water concentration in the coagulation bath significantly exceeded 20% (v/v).

Although strength and stiffness data are presented here as a function of fiber diameter (Figure 2), it is expected that the draw ratio is the primary factor influencing the mechanical properties. This is confirmed by the observation that, when extrapolated to the same diameter, fibers spun from large spinnerets (i.e., extended to a larger draw ratio) show better mechanical properties than specimens produced with a smaller spinneret (insets in Figure 2). On the other hand, fibers spun with spinnerets of different sizes and then subjected to the same postspinning processing have essentially identical mechanical properties independent of d. This shows that the spinneret size hardly affects the fiber properties and that the plot of mechanical behavior as a function of final fiber diameter gives clear results only for a constant spinneret size.

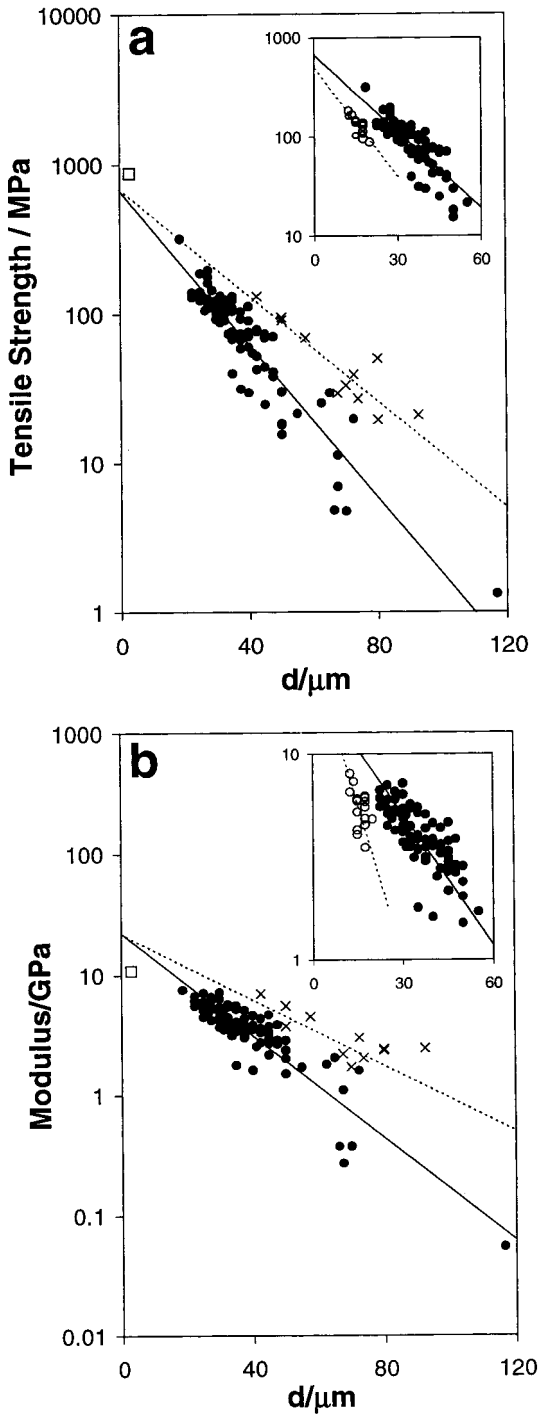

Figure 2. Postspinning processing improves mechanical fiber properties. Tensile strength (a) and modulus (b) of regenerated spider silk as a function of the diameter of the processed fiber. Main figures show data of fibers spun through a spinneret with 250 μm i.d. using pure acetone (●) and a mixture of 5% (v/v) water in 95% (v/v) acetone (×) as coagulant media. Tensile data of specimens obtained with different postspinning processing schemes are not distinguished by use of different symbols. Data of the native silk are included in the figure (□). Smaller insets compare properties of fibers spun into pure acetone using spinnerets with 150 μm (○) and 250 μm (●) inner diameter.

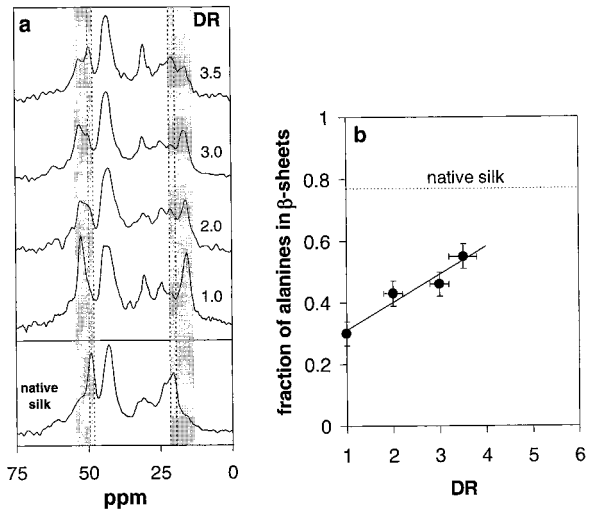

Figure 3. Postspinning drawing affects fiber structure. (a) ^{13}C CP/MAS NMR spectra of single-drawn regenerated spider silk samples (air-dried and annealed) as compared to the spectrum of native silk. Shaded areas highlight the chemical shift ranges of C_α and C_β carbons of alanine in proteins. Regions between dotted lines are typical of those alanine residues adopting the β-sheet conformation. (b) Fraction of alanine residues adopting the β-sheet conformation, as determined by deconvolution of the 14−22 ppm region of the spectra shown in (a).

Protein Structure. Macroscopic properties of fibers depend on their crystallinity, three-dimensional polymer architecture, and overall degree of molecular orientation.[24] Hence, it is expected that the observed improvements of the mechanical properties of our regenerated spider silk fibers by postspinning processing are due to processing-induced modifications of the material on a molecular level, though the reduction of the fiber porosity, described above, will also contribute. Stress-, thermal-, and solvent-induced changes of the microscopic properties of silk materials have already been repeatedly observed.[1,19−21,25−27]

We have investigated the influence of the first drawing step on the fiber structure by means of solid-state NMR spectroscopy. For this purpose, ^{13}C cross-polarization magic angle spinning (CP/MAS) NMR spectra were acquired for a series of single-drawn regenerated silk samples, differing only in the extent of the postspinning draw applied to the fibers.^{13}C NMR is a commonly used technique to investigate the secondary structure of silks and silk-fibroin materials.[20,21,25,27,28] A simple diagnostic test exploits the dependence of the isotropic chemical shift of ^{13}C atoms on the local conformation of the protein.[28] In our silks, drawing-induced changes in the ^{13}C CP/MAS NMR spectra are particularly observed in the chemical shift regions at 14−22 and 48−53 ppm (shaded areas in Figure 3a). These spectral regions correspond respectively to the C_β and C_α carbons of alanine. ^{13}C NMR studies of silks often focus on these resonances for a variety of reasons. Not only is alanine a major constituent of most silky materials, it is also generally presumed that the alanine-rich segments of the silk proteins are primarily associated with the crystalline regions of the silk responsible for its high strength.[3,14,29] Conveniently, the NMR signature of the alanine C_β carbons does not overlap with other spectral resonances, so unambiguous experiments can be carried out without site-selective ^{13}C enrichment. Furthermore, the relationship between the chemical shifts of these signals and the local protein structure is well established, and the chemical shift dispersion is exceptionally large.[27,28]

Deconvolution of the alanine C_β regions of the spectra shown in Figure 3a is possible if we account for components at 16 ppm (assigned to the C_β carbons of alanines in either helical structures or random coils), at 21 ppm (the C_β carbons of alanines in β-sheet structures), and at 24 ppm (side chain carbons of either leucines or arginines). The fraction of alanines in β-sheet structures, which is determined by this procedure, increases linearly with the extent of drawing applied to the specimen (Figure 3b). Thus, the drawing-induced improvement of the mechanical properties of the regenerated silk appears to be, at least in part, due to a reinforcement of the fibers by very strong and stiff poly(alanine) microcrystallites—as they have previously been associated with the high strength and stiffness of the native silk as well.[3,29] Though the fraction of alanine residues found in β-sheet structures can be almost doubled in a single postspinning drawing step, the very high value of the native silks is not achieved. If the fraction of alanine residues in β-sheets is linearly related to the initial draw ratio, it would appear necessary to apply draw ratios greater than 6 to produce a regenerated fiber with the same fraction found in the native silk (see Figure 3b).

We have further addressed the question of how subsequent treatment of the regenerated silk with water affects its micro- and macroscopic properties. Soaking a single-drawn material in water for 4 h, with the fiber ends unconstrained, results in a large increase in the fraction of alanine residues adopting the β-sheet conformation (Figure 4a). The NMR spectrum of the water-treated material is nearly identical with that of the native silk. A similar observation has previously been found when an as-spun regenerated fiber was soaked in water.[21] The observed structural reorganization of the protein is associated with the reduction of its polymer glass transition temperature in the presence of water. In our recent studies we have shown that water acts as a silk plasticizer; i.e., it significantly increases the mobility of the hydrophilic segments of the molecular strands in spider dragline silk fibroin.[30] The segmental main chain mobility makes kinetically possible molecular reorganization of the silk protein. Because of the dense packing of amino acid residues in β-sheet crystals, this structure is thermodynamically favored by the hydrophobic poly(alanine) runs if the silk is in contact with water. Surprisingly, the water-induced change in the microscopic fiber structure leads to no significant modification of the macroscopic material properties. While a high concentration of β-sheets composed of alanine residues appears to be a necessary condition for good tensile behavior, it is not in itself sufficient.

Double-drawn fibers, i.e., specimens drawn in water after being prestretched in air, also exhibit a high fraction of alanine adopting the β-sheet conformation (Figure 4b). Though this fraction approaches 65%, it is still lower than in the native silk (77%). While increasing the total draw ratio in the two-step drawing process from 3 to 7 does not result in a major change of the NMR signature of the processed material (Figure 4b), the mechanical properties of the fiber show further improvement. Hence, an additional factor or factors must be critical in establishing the material's tensile behavior.

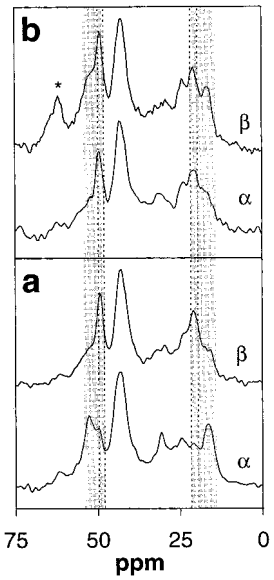

Figure 4. Postspinning water treatments affect fiber structure. (a) Comparison of ^{13}C CP/MAS NMR spectra of a single-drawn regenerated silk fiber (DR = 3) before (α) and after (β) being soaked in water for 4 h. Samples have been air-dried and annealed before the investigation. (b) Spectra of regenerated silk fibers (air-dried and annealed) that have been drawn in air and subsequently in water in a two-step process (α: $DR_1 = 2$, $DR_2 = 1.5$; β: $DR_1 = 3.5$, $DR_2 = 2$). The latter specimen is ^{13}C-labeled at the carbonyl position of the alanine residues. The signal marked with an asterisk contains signal contributions of a rotational sideband of the carbonyl carbon signal at 172 ppm whose intensity is greatly enhanced compared to those of the other spectra due to the isotopic enrichment. The ^{13}C enrichment does not affect the spectral region of the alanine C_β carbons.

Molecular Orientation and Crystalline Structure. The crystallinity and degree of molecular orientation determine the tensile properties of synthetic fibers.[24] A high degree of molecular orientation in both the crystalline and the amorphous domains of native spider dragline silk has previously been demonstrated.[14,31] The nature and size of the crystals in a semicrystalline material also affect its properties. All of these factors can be explored by wide-angle X-ray diffraction. Figure 5 shows WAXD patterns of regenerated spider silk specimens (a−c) and compares them to the pattern of the native silk (d). Figure 6 shows radial intensity scans along the equator of each of these patterns.

The X-ray results reveal the strong structural similarity between the as-spun and single-drawn regenerated silks. Like silk fibroin that was freeze-dried from formic acid solution,[32] both fibers show broad features at *d*-spacings ($d = 1/s$) of 4.4 and 8.1 Å. The origin of the inner reflection (8.1 Å) as yet remains unclear. It matches neither the *d* spacings typical of β-sheets nor the 7.4 Å spacing found for the α-helical structures in α-poly(L-alanine).[33] The position and width of the outer (4.4 Å) ring are identical to those of the noncrystalline phase in natural spider silk. This is considered to consist of both truly amorphous material and isolated or poorly stacked β-folded sheet structures. The double-drawn regenerated silk, like the native silk, exhibits two narrower diffraction rings at *d*-spacings of 5.6 and 4.6 Å. On the basis of a comparison with original data of Warwicker,[34] these have previously been assigned to diffraction at the (200) and (120) planes, respectively, of pseudo-orthorhombic poly(alanine) microcrystals containing β-pleated sheets.[31] In contrast to the diffraction pattern of the native silk, the double-drawn regenerated fiber exhibits an additional halo at $s \approx 1.1$ nm^{-1} ($d \approx 9$ Å) that may be a residue of the unidentified disordered phase seen in the as-spun and single-drawn fibers.

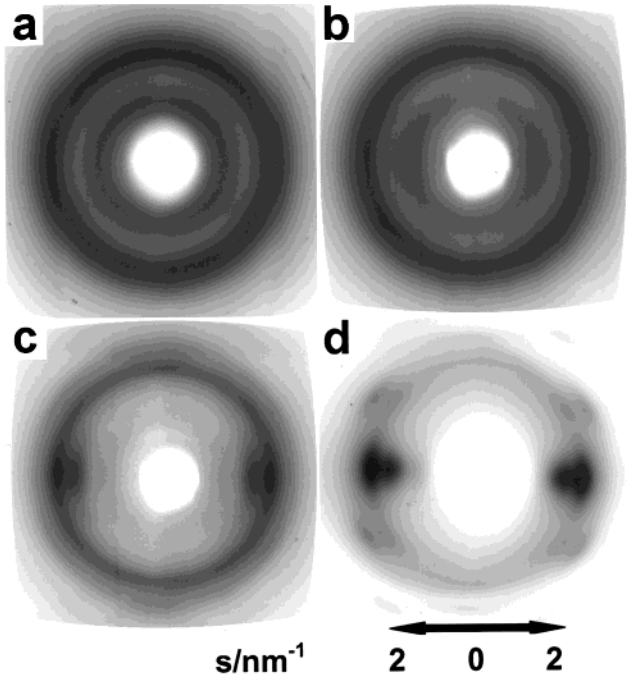

Figure 5. Crystallinity and molecular orientation in regenerated and native spider silks. WAXD patterns of (a) an as-spun regenerated fiber, (b) a single-drawn regenerated fiber (DR = 3.5), (c) a double-drawn regenerated fiber ($DR_1 = 3.5$, $DR_2 = 2$), and (d) native silk. The investigated regenerated fibers were air-dried but not annealed.

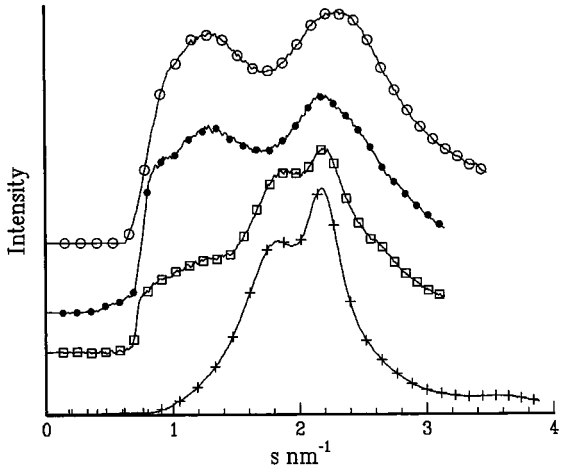

Figure 6. Radial intensity scans along the equator of the patterns shown in Figure 5 (shifted vertically for clarity): (○) as-spun regenerated silk, (●) single-drawn regenerated silk, (□) double-drawn regenerated silk, (+) natural spider silk.

From these results, we conclude that three-dimensional poly(alanine) crystals with β-sheet structure are formed only during the second drawing step—despite the increase in the fraction of alanine residues adopting β-sheet conformation, as observed by NMR, after the first stage of drawing (see previous section and Figure 3). In synthetic and/or semicrystalline polymers, drawing conditions can be found that cause the crystal size to either increase or decrease, as the reorientation under

draw allows small groups of bound atoms the freedom to find conformations of low energy. The observed increase in β-sheet fraction after the second stage of drawing should correspond to more efficient stacking of individual sheets which were originally isolated into three-dimensional crystallites. We believe that the presence of water which increases local mobility in the protein promotes this reorganizational process. While this ordering process does not increase the β-sheet fraction of alanine probed by NMR, the more efficient reinforcement does result in improved tensile properties of the fiber.

Qualitative inspection of the X-ray patterns in Figure 5 reveals no preferential molecular orientation in the as-spun fibers and only very small degree of orientation in the single-drawn fibers. Both samples show diffraction rings with almost constant intensity (Figure 5a,b). In contrast, both regenerated silkworm silk fibers[19] and fibers spun from a spider silk analogue protein[8,12] have been reported to show significant degrees of molecular orientation even at small draw ratios. We as yet cannot comment on reasons for the different behavior of the three fibers spun from similar proteins (i.e., regenerated silkworm silk, regenerated spider dragline silk, and fibers from a silk analogue protein). In regenerated spider silk, significant crystal alignment parallel to the fiber axis is found only as it is stretched in water in a second step, i.e., at comparatively large total draw ratios (Figure 5c). In Figure 5c there appear features on the meridian and at the position of the first layer line of the normal silk structure (as shown in Figure 5d). These diffuse reflections correspond to poorly oriented crystals with the normal silk crystal structure, and each feature is observed as a sharp, more strongly oriented feature in Figure 5d. Still, even after the second drawing stage, the regenerated silk exhibits less overall orientation than the native material, indicating that in the regenerated silk a fraction of the material is well-ordered but unoriented. No such phase exists in the native silk.

Conclusions

Four factors of importance for the tensile properties of regenerated spider dragline silk fibers have been identified, namely, (a) its porosity, (b) the fraction of alanine residues adopting the β-sheet conformation, (c) the extent of its crystallinity, and (d) its overall degree of molecular orientation. These parameters are determined by the sample's postspinning processing history, especially by the extent of draw applied to the fiber. Water can plasticize the silk fibroin and, hence, stabilizes postspinning drawing processes and facilitates protein crystallization. The future success of any rational design of artificial protein materials will depend on the generalizibility of fundamental studies such as the present one.

Acknowledgment. This work was funded through NSF Grants DMR-9708062 and MCB-9601018 and through seed funding provided by the Cornell Center for Materials Research under NSF Grant DMR-9632275. A.S. acknowledges financial support through a postdoctoral fellowship by the DFG while O.L. thanks support from the NIH Training Grant in Molecular Physics of Biological Systems.

References and Notes

(1) *Biomaterials: Novel Materials from Biological Sources*; Byrom, D., Ed.; Stockton Press: New York, 1991.
(2) Bunning, T. J.; Jiang, H.; Adams, W. W.; Crane, R. L.; Farmer, B.; Kaplan, D. In *Silk Polymers: Materials Science and Biotechnology*, ACS Symposium Series 544; Kaplan, D., Adams, W. W., Farmer, B., Viney, C., Eds.; American Chemical Society: Washington, DC, 1994; Chapter 29.
(3) Jelinski, L. W. *Curr. Opin. Solid State Mater. Sci.* **1998**, *3*, 237−245.
(4) Xu, M.; Lewis, R. V. *Proc. Natl. Acad. Sci. U.S.A.* **1990**, *87*, 7120−7124.
(5) Hinman, M. B.; Lewis, R. V. *J. Biol. Chem.* **1992**, *267*, 19320−19324.
(6) Colgin, M. A.; Lewis, R. V. *Protein Sci.* **1998**, *7*, 667−672.
(7) Prince, J. T.; McGrath, K. P.; DiGirolamo, C. M.; Kaplan, D. L. *Biochemistry* **1995**, *34*, 10879−10885.
(8) O'Brien, J. P.; Fahnestock, S. R.; Termonia, Y.; Gardner, K. H. *Adv. Mater.* **1998**, *10*, 1185−1195.
(9) Fahnestock, S. R.; Irwin, S. L. *Appl. Microbiol. Biotechnol.* **1997**, *47*, 23−32.
(10) Fahnestock, S. R.; Bedzyk, L. A. *Appl. Microbiol. Biotechnol.* **1997**, *47*, 33−39.
(11) Arcidiacono, S.; Mello, C.; Kaplan, D. *Appl. Microbiol. Biotechnol.* **1998**, *49*, 31−38.
(12) Fahnestock, S. R. Novel, recombinantly produced spider silk analogs. Int. Application # PCT/US94/06689, Int. Publication # WO 94/29450, 1994.
(13) Jelinski, L. W.; Blye, A.; Liivak, O.; Michal, C.; LaVerde, G.; Seidel, A.; Shah, N.; Yang, Z. *Int. J. Biol. Macromol.* **1999**, *24*, 197−201.
(14) Simmons, A. H.; Michal, C. A.; Jelinski, L. W. *Science* **1996**, *271*, 84−87.
(15) Michal, C. A.; Jelinski, L. W. *J. Biomol. NMR* **1998**, *12*, 231−241.
(16) Cohen, P. *New Sci.* **1998**, *160*, 11.
(17) Cappello, J.; McGrath, K. P. In *Silk Polymers: Materials Science and Biotechnology*, ACS Symposium Series 544; Kaplan, D., Adams, W. W., Farmer, B., Viney, C., Eds.; American Chemical Society; Washington, DC, 1994; Chapter 26.
(18) Lock, R. L. *Process for making silk fibroin fibers*. US Patent 5,252,285, 1993.
(19) Trabbic, K. A.; Yager, P. *Macromolecules* **1998**, *31*, 462−471.
(20) Liivak, O.; Blye, A.; Shah, N.; Jelinski, L. W. *Macromolecules* **1998**, *31*, 2947−2951.
(21) Seidel, A.; Liivak, O.; Jelinski, L. W. *Macromolecules* **1998**, *31*, 6733−6736.
(22) Zemlin, J. C. Technical Report TR69-29-CM (AD684333), US Army Natick Laboratories, Natick, MA, 1968.
(23) Cunniff, P. M.; Fossey, S. A.; Auerbach, M. A.; Song, J. W.; Kaplan, D. L.; Adams, W. W.; Eby, R. K.; Mahoney, D.; Vezie, D. L. *Polym. Adv. Technol.* **1994**, *5*, 401−410.
(24) *The strength and stiffness of polymers*; Zachariades, A. E., Porter, R. S., Eds.; Marcel-Dekker: New York, 1983.
(25) Ishida, M.; Asakura, T.; Yokoi, M.; Saito, H. *Macromolecules* **1990**, *23*, 88−94.
(26) Tsukada, M.; Gotoh, Y.; Nagura, M.; Minoura, N.; Kasai, N.; Freddi, G. *J. Polym. Sci., Part B: Polym. Phys.* **1994**, *32*, 961−968.
(27) Saito, H.; Tabeta, R.; Asakura, T.; Iwanaga, Y.; Shoji, A.; Ozaki, T.; Ando, I. *Macromolecules* **1984**, *17*, 1405−1412.
(28) Saito, H. *Magn. Reson. Chem.* **1986**, *24*, 835−852.
(29) Termonia, Y. *Macromolecules* **1994**, *27*, 7378−7381.
(30) Yang, Z.; Liivak, O.; Seidel, A.; LaVerde, G.; Zax, D. B.; Jelinski, L. W., submitted for publication.
(31) Grubb, D. T.; Jelinski, L. W. *Macromolecules* **1997**, *30*, 2860−2867.
(32) Grubb, D. T.; Jackrel, D., unpublished results.
(33) Bamford, C. H.; Brown, L.; Elliot, A.; Hanby, W. E.; Trotter, I. F. *Nature* **1954**, *173*, 27−29.
(34) Warwicker, J. O. *J. Mol. Biol.* **1960**, *2*, 350−362.

MA990893J